

Numerical study towards closed fish farms in waves using two Harmonic Polynomial Cell methods

Yugao Shen^{*1}, **Marilena Greco**^{1,2}, **Odd M. Faltinsen**¹, **Shaojun Ma**¹

¹ NTNU AMOS, Marine Technology Department, NTNU, Trondheim, Norway

² CNR-INM, Institute of Marine Engineering, Roma, Italy

* yugao.shen@ntnu.no

In order to avoid salmon lice and minimize environmental pollution, closed fish-farm concepts are gaining increasing attention in Norway. Violent sloshing of the water inside the closed cage then becomes an important issue affecting structural and mooring loads. The main objective of our ongoing study is to develop a numerical tool to predict the response of a moored closed fish farm in waves. As a part of the solution-strategy development, here we will examine a simplified case: a two-dimensional (2D) closed fish farm.

External flow model: The sway motion of a body with rectangular cage(s) in regular incident waves with 2D flow is considered. The body is restrained from oscillating in heave and roll. Transient linear potential-flow effect is included based on the convolution integral to account for possible high-order nonlinear components induced by the sloshing force on the body motions. The motion equation for sway is given as

$$(M + A_{22}^{\infty})\ddot{\eta}_2 + B_{22}^{visc} \dot{\eta}_2 |\dot{\eta}_2| + C_{22}\eta_2 + \int_0^t k_{22}(\tau)\dot{\eta}_2(t-\tau)d\tau = F_2^{exc} + F_2^{slosh} \quad (1)$$

Here M is the structural mass (excluding liquid mass), A_{22}^{∞} is the infinite-frequency sway added mass and $k_{22}(t)$ is the retardation function associated with the external flow. B_{22}^{visc} represents viscous damping for external flow, C_{22} is the linear spring coefficient, F_2^{exc} is the horizontal linear wave excitation force, and F_2^{slosh} is the horizontal force caused by internal sloshing. The hydrodynamic coefficients and the wave excitation force associated with the external flow are solved by a linear potential-flow frequency-domain solver based on a Boundary Element Method (BEM).

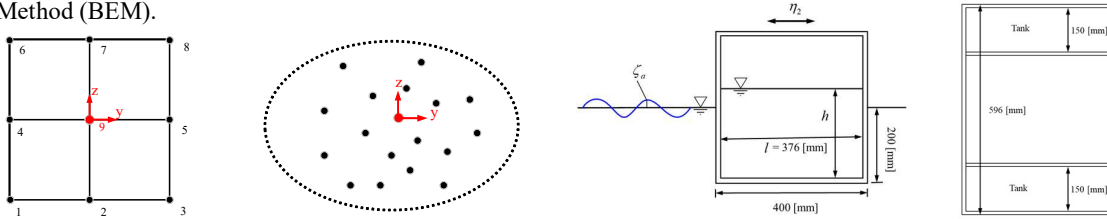


Fig. 1 Left two plots: regular cell and irregular cells for HPCell method. Right two plots: side and top view of the experimental set-up from Rognebakke and Faltinsen [1].

Internal flow model: To estimate the sloshing force F_2^{slosh} , the internal potential flow is solved using the harmonic polynomial cell (HPCell) method. The essence of this method is that the Laplace equation is automatically satisfied by the chosen harmonic polynomials. The problem is solved in a tank-fixed coordinate system with body boundary and nonlinear free-surface conditions. In the present paper, two types of cells are adopted. One is the standard harmonic polynomial cell method with quadrilateral cells (HPCell-Reg), which was originally proposed by Shao and Faltinsen [2, 3] and has been further developed by other researchers, for instance by Hanssen et al. [4] and Ma et al. [5]. The computational domain is divided into overlapping quadrilateral cells, each with eight boundary nodes numbered as 1-8 (see left plot of Fig.1). The velocity potential of a given point (y, z) inside a cell can be represented as a linear combination of harmonic polynomials f_j , i.e.,

$$\varphi(y, z) = \sum_{j=1}^n b_j f_j(y, z) \quad (2)$$

Here n is the number of polynomials used and $n = 8$ for HPCell-Reg. By enforcing eq. (2) at the eight boundary nodes, the unknown coefficients b_j can be readily obtained as a linear combination of the nodal velocity potentials φ_i ($i = 1, 2, \dots, 8$). The harmonic polynomials up to fourth-order are included, leading to a spatial accuracy of φ between 3rd and 4th order. For cases with steep free-surface profile, the accuracy of HPCell-Reg may decrease rapidly due to low-quality/distorted stencils. Wang et al. [6] proposed a so-called “irregular cell” technique for accurate discretization of Laplace equation with polynomials (HPCell-Irreg) in scenarios where it is difficult to construct high-quality stencil. Each irregular cell consists of a center point and its neighboring points (see middle left plot of Fig.1). To reach the accuracy of order k , the first $n = 2k + 1$ polynomials need to be selected. By applying eq. (2) at all the neighboring positions, we can obtain a linear equation system for the unknown coefficients b_j . To guarantee that the obtained equations are solvable, the number of neighboring points should be sufficiently larger than $2k + 1$. To have enough neighboring points, local refinement of the grid is favorable. The equations then can be solved by the least-square method. The HPCell-Irreg has great freedom to choose the order of the harmonic polynomials and to select neighboring points. One of the disadvantages of the HPCell-Irreg is that

more non-zeros will be in the global coefficient matrix, leading to lower computational efficiency. Here, when applying HPCell-Reg, the free surface is modelled as an immersed boundary in a Cartesian grid with square cells. The free surface is tracked by following the markers. The markers are tracked in a semi-Lagrangian way which means that markers can only move along vertical gridlines. A 4th order Runge-Kutta scheme is chosen to march the solution in time. Nonlinear free-surface kinematic and dynamic boundary conditions are enforced on the free-surface markers. An artificial damping term $-\mu\varphi$ is also included in the dynamic free-surface condition, accounting for the viscosity due to the internal boundary-layer flow. For HPCell-Irreg, the basic procedure is similar as that of HPCell-Reg, except that irregular cells are constructed in domains where square cells are difficult to be implemented. The free-surface markers are tracked in a semi-Lagrangian or in a Lagrangian way when wave overturning happens. If the angle of the free surface at the tank wall is very small, the computational domain is truncated by introducing a horizontal cut at the wall (Zhao and Faltinsen [7]).

Case 1: sloshing inside a forced oscillatory rectangular tank

The sloshing inside a 2D rectangular tank undergoing forced harmonic sway oscillations is investigated to check the robustness of the above two HPCell methods. The mean filling water depth is $h = 0.186\text{m}$ and the tank breadth is $l = 0.376\text{m}$. The corresponding largest natural sloshing period is $T_n = 0.727\text{s}$. The internal damping μ is 0.3% of the critical damping for the lowest mode according to Faltinsen and Timokha [8]. The tank is forced to oscillate in the horizontal direction with period $T = 8\text{s}$ and two amplitudes $\eta_{2a}/l = 0.001/0.376$ and $0.004/0.376$, respectively. Numerical results from HPCell-Reg and HPCell-Irreg are provided and compared against those from the multimodal method. The latter is a weakly non-linear analytical method with one dominant mode proposed by Faltinsen and Timokha [8]. Our focus will be on the wave elevation ζ at the left tank wall and the sloshing induced horizontal force F_2^{slosh} . Fig. 2 shows the comparison of the wave elevation (left) and the horizontal sloshing force (right) from the different methods with forced oscillation sway amplitude $\eta_{2a}/l = 0.001/0.376$. From the figure, nice agreement is achieved for both variables from all the three methods.

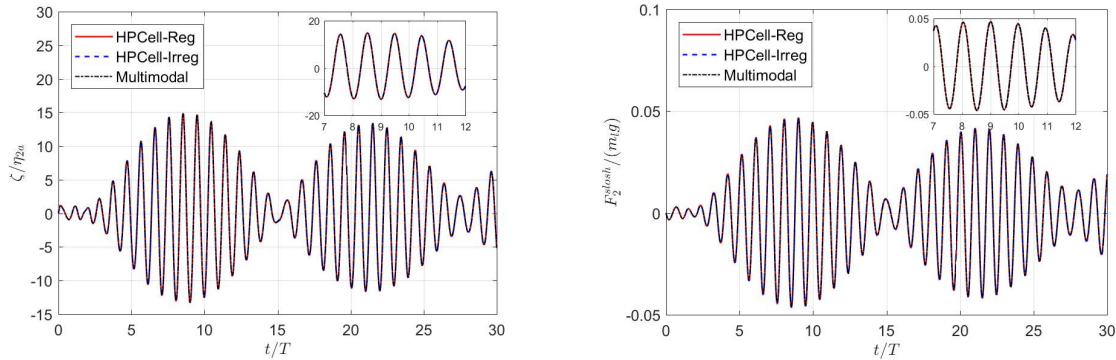


Fig. 2 Case 1: forced oscillation amplitude $\eta_{2a}/l = 0.001/0.376$. Left: non-dimensional wave elevation. Right: non-dimensional sloshing force with m_1g the weight of the internal liquid. A zoomed view is also given near the absolute maximum value of the variables. Results from HPCell-Reg, HPCell-Irreg and multimodal method.

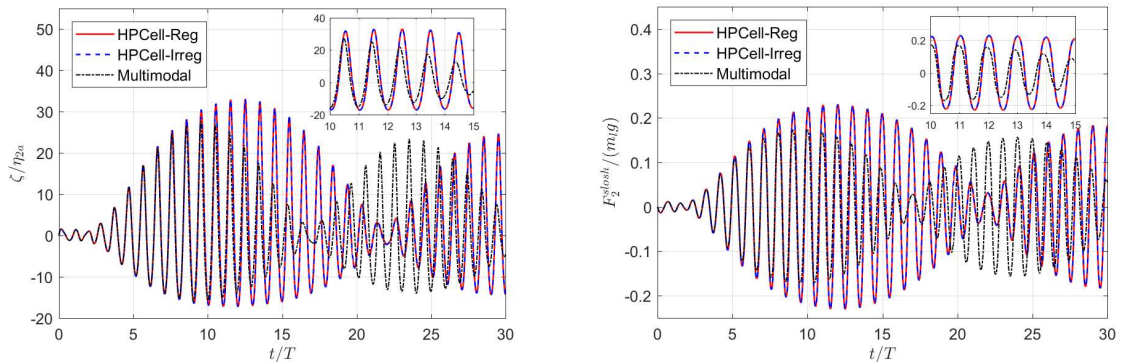


Fig. 3 Same as in Fig.2, but for oscillation amplitude $\eta_{2a}/l = 0.004/0.376$.

The comparison for the case with larger oscillation amplitude, i.e., $\eta_{2a}/l = 0.004/0.376$ is presented in Fig. 3. The figure shows that the wave elevation and the sloshing force from HPCell-Reg and HPCell-Irreg match well during the whole simulation with small differences in the local peaks. The results from the multimodal method agree nicely with the HPCell methods at the initial stage ($t < 10T$) when the wave amplitude is relatively small, but larger discrepancy is observed as the wave amplitude increases. Fourier analysis of the wave elevation shows that the first and second Fourier modes are of similar magnitude after the initial stage. This violates the assumption of

the applied multimodal method, i.e., the first sloshing mode should be dominant. A multimodal method with more than one dominant mode will be investigated.

Case 2: a rectangular-shaped closed cage freely floating in waves

A body with constant cross-section containing either one or two rectangular shaped tanks in regular waves was numerically investigated and compared with the experimental results by Rognebakke and Faltinsen [1]. The experimental set-up is shown in the right two plots of Fig.1. The body length was nearly equal to the width of the wave flume. Four strips of glass were added onto the end plates to assure a low flow of water past the ends of the body, ensuring nearly 2D flow conditions. The body is only allowed to move in sway. Three scenarios are investigated with empty tank, one tank and two tanks filled. Depending on the number of tanks filled and the filling water depth h , the structural mass M of the cage is varied to keep the mean water draft equal to 0.2 m. As a rough estimation of B_{22}^{visc} , the drag coefficient $C_D = 3$ is used, corresponding to a facing square in infinite fluid. Numerical results show that the steady-state sway motion is not sensitive to C_D . The tank filling depth is $h = 0.184$ m and the breadth is $l = 0.376$ m. The lowest natural frequency $\omega_n = 8.65$ rad/s.

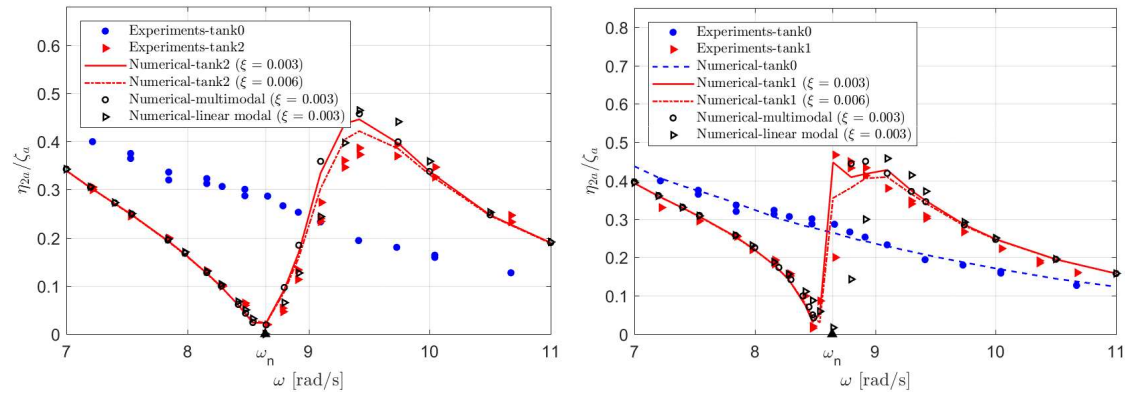


Fig. 4 Case 2: experimental (from [1]) and numerical wave-induced steady-state sway motion amplitude η_{2a} , made non-dimensional by the incident wave amplitude ζ_a . Tank0, tank1 and tank2 denote empty tank, one tank and two tanks filled, respectively. The filled-tank numerical results are based on two different damping ratios ξ . Numerical results based on linear sloshing model and nonlinear multimodal method from [8] are also included.

Comparisons between the numerical and experimental results for the steady-state amplitude of sway motion η_{2a} are presented in Fig. 4. Since the sway motion is nonlinear, the amplitude η_{2a} is calculated as (peak value – trough value)/2. HPCell-Reg is used for most of the frequencies except those in the resonance region where HPCell-Irreg is applied because of break-down of the HPCell-Reg simulations and low-quality stencil. The figure shows that the numerical predictions are, in general, in good agreement with the experimental results for all the examined scenarios with largest differences in the resonance region. There are two very different measured sway amplitudes for a wave frequency $\omega = \omega_n$ (see left plot of Fig.4) for the case with one tank. This could be similar to the jumps between different branches of the steady-state sloshing solution when a tank is subjected to forced oscillations (see [8]). When the two tanks are filled (see right plot of Fig.4), the sway amplitude has a minimum at $\omega = \omega_n$ and maximum sway amplitude occurs at a frequency higher than ω_n . The above results denote that varying the number of filled tanks may lead to totally different results. For the internal damping, it is $\xi = 0.3\%$ of the critical damping, according to [8]. Results with $\xi = 0.6\%$ are also included for comparison. Negligible influence is observed for the two ξ except for the resonance zone of sway motion, where $\xi = 0.6\%$ leads to slightly better results. When performing simulations with one tank, the motion of the body is clearly dependent on the damping ratio ξ for wave frequencies in the vicinity of ω_n . This could be related to the jump behavior introduced above. The internal flow can be with strong nonlinearities in the resonance zone. Snapshots of the free-surface profile at different time instants are shown in Fig. 5 for wave frequency $\omega = 8.8$ rad/s as an indication of free-surface nonlinearities in the resonance zone.

Numerical simulations with sloshing solved by the linear modal method and the nonlinear multimodal method from [8] are performed and the corresponding results are also shown in Fig. 4. The linear modal method is commonly used in engineering practice for solving sloshing problems. Numerical results show that the linear model can give a reasonable prediction of the cage motion for the case with two tanks, but erroneous results are obtained in the resonance region when one tank is filled. The multimodal method can provide comparable results with the HPCell methods for both cases, but with much less computational time, so it is promising for future analysis of the cage in stochastic sea.

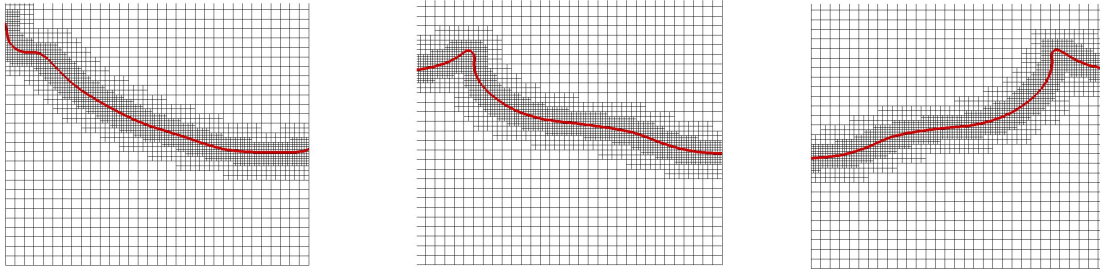


Fig. 5 Snapshots of the free-surface profile at three time instants by HPCell-Irreg.

To see more clearly the interactions between the internal sloshing and the body motion, a Fourier analysis of the time histories of the sloshing force and the sway motion are performed for the case with incident wave period $T = 8$ s, wave amplitude $\zeta_a = 0.02$ m and one tank filled. From the analysis of the steady-state sway motion, there is one dominant component with the frequency equals the incident wave frequency. The above analysis indicates that the floating system seems to be able to filter out the contributions from the super-harmonic sloshing force components and reduce the internal sloshing severity compared with the forced oscillatory scenario. Rognebakke and Faltinsen [1] presented also a case with intermediate water depth. The experiments and our numerical simulation indicate more violent sloshing and needs to be further studied.

Conclusions

Description of free-surface elevation during violent sloshing requires high numerical accuracy. The presented HPCell methods show promising results. When describing the interaction between sloshing and body motions, the free-surface details are not as important as for forced oscillations. However, free-surface nonlinearities matter and can reasonably be described by the multimodal method in the studied cases. Future studies of mooring and structural loads on a closed fish cage in a stochastic sea must pay attention to computational time. The nonlinear multimodal method has an advantage in this context. It is also needed for the mooring loads to include weakly nonlinear difference-frequency exterior flow effects.

Acknowledgements

This work has been carried out at the Centre for Autonomous Marine Operations and Systems (NTNU AMOS) and supported by the Research Council of Norway through the Centre of Excellence funding scheme, Project number 223254- AMOS.

References

- [1] Rognebakke, O. F., & Faltinsen, O. M. (2003). Coupling of sloshing and ship motions. *Journal of Ship Research*, 47(3), pp.208-221.
- [2] Shao, Y. L., & Faltinsen, O. M. (2012). Towards efficient fully-nonlinear potential-flow solvers in marine hydrodynamics. In *ASME 2012 31st International Conference on Ocean, Offshore and Arctic Engineering* (pp. 369-380). American Society of Mechanical Engineers.
- [3] Shao, Y. L., & Faltinsen, O. M. (2014). A harmonic polynomial cell (HPC) method for 3D Laplace equation with application in marine hydrodynamics. *Journal of Computational Physics*, 274, 312-332.
- [4] Hanssen, F. C., Bardazzi, A., Lugni, C., & Greco, M. (2018). Free-surface tracking in 2D with the harmonic polynomial cell method: Two alternative strategies. *International Journal for Numerical Methods in Engineering*, 113(2), 311-351.
- [5] Ma, S., Hanssen, F. C., Siddiqui, M. A., Greco, M., & Faltinsen, O. M. (2018). Local and global properties of the harmonic polynomial cell method: In-depth analysis in two dimensions. *International Journal for Numerical Methods in Engineering*, 113(4), 681-718.
- [6] Wang, J., Faltinsen, O. M., & Duan, W. (2020). A high-order harmonic polynomial method for solving the Laplace equation with complex boundaries and its application for free-surface flows. Part I: two-dimensional cases. Submitted for publication.
- [7] Zhao, R., & Faltinsen, O. M. (1993). Water entry of two-dimensional bodies. *Journal of Fluid Mechanics*, 246, pp.593-612.
- [8] Faltinsen O. M., & Timokha A. N. (2009). *Sloshing*. New York: Cambridge University Press.